Application Note

Cell Migration and Invasion

Agilent
Trusted Answers

Combination of a Fluorescent Substrate-Based MMP Activity Assay and Hit Pick Reading/Imaging Procedure

Efficiently screen for inhibitors of MT1-MMP activity and 3D glioma tumoroid invasion

Authors

Brad Larson
Agilent Technologies, Inc.

Ania Knapinska, and Gary Drotlef
Institute for Human Health and Disease Intervention (I-HEALTH)
Florida Atlantic University
Alphazyme

Gregg Fields
Institute for Human Health and Disease Intervention (I-HEALTH)
Florida Atlantic University
Department of Chemistry
The Scripps Research Institute
Scripps Florida

Abstract

Malignant gliomas are the most common primary brain tumors in the United States. Membrane type 1 matrix metalloproteinase (MT1-MMP) has been shown to be crucial for the progression, invasion, migration, and angiogenesis of tumors. Use of a fluorescent substrate to quantify MT1-MMP activity, where tumoroids are embedded in a collagen hydrogel, would simplify detection of potential protease inhibitors, while using an *in vivo*-like cell model. When substrate and experimental setup are combined with the hit pick joint reading and imaging process available in Agilent BioTek Gen5 microplate reader and imager software, the most efficient inhibitor screening method is created. It saves time and image storage needs by only imaging wells with test molecules that demonstrate inhibitory effects.

Introduction

Malignant and nonmalignant brain tumors are composed of a group of more than 100 different types. Malignant gliomas, including glioblastoma multiforme (GBM) and astrocytomas, are the most common primary brain tumors in the United States[1], and make up 78% of malignant brain tumors.[2] Although relatively rare, particularly in the US, malignant brain tumors exhibit a disproportionate cancer mortality due to their high fatality rates; where on average, only one-third of individuals survives at least five years after diagnosis.[3] MT1-MMP (also known as MMP-14) has been shown to be crucial for the progression, invasion, migration, and angiogenesis of tumors.[4,5] MT1-MMP belongs to a subset of zinc-dependent membrane-anchored MMPs, which are able to degrade the basement membrane and proteins of the extracellular matrix (ECM)[6], cell adhesion molecules, cytokines, growth factors, and receptors.[7] Its expression also correlates with tumor grade and is associated with reduced survival in gliomas.[8,9] Therefore, many studies have highlighted its potential as a therapeutic target in many cancers.[10,11]

Invasion is considered one of the main hallmarks of cancer[12,13], and is the result of continuous interaction between tumor cells and the surrounding microenvironment.[12-14] When glioma cells invade through the brain parenchyma, they establish contact with molecules of the ECM and components of the basement membrane. As part of this process, surface proteases, such as MT-MMPs, are recruited at the focal contacts with the ECM where, either directly or indirectly (through the activation of soluble matrix metalloproteases), they degrade and remodel the surrounding ECM, favoring invasion.[15] For many years, the simplest model to study cell motility, especially with respect to cell to ECM interactions, consisted of culturing cells in a two-dimensional (2D) monolayer on glass, plastic slides, or microplates.[16] ECM components were used either as a coating, or solubilized in the medium, and the assay involved the observation of motility.[16] Despite the simplicity of the model, there were numerous limitations[16]; in particular, the assay monitored motility and not invasion.[17] It also did not take into account the fact that cells in monolayers behave differently than cells cultured in a three-dimensional (3D) manner.[18, 19] Because of this limitation, newer and more advanced cell models have been developed to better mimic the *in vivo* cell environment. A particular model that shows promise incorporates round-bottom spheroid microplates, where tumor-specific primary cells or cultured cell lines are added to plate wells. Following aggregation, the 3D tumor models are embedded in a hydrogel, such as collagen or Matrigel, and allowed to invade the ECM. This type of model allows for complex development, which more closely mimics tumor development[20], and gives rise to tumors resembling the *in vivo* invasion pattern of the tumor of origin.[20] It has also been demonstrated that this 3D invasion model leads to increased production of matrix-degrading enzymes, such as matrix metalloproteinases[21, 22], and is more predictive of therapy response.[23]

Incorporation of 3D cell models has been proven to deliver results more indicative of an *in vivo* response. However, when cellular imaging is included to determine the effect of potential test molecules, this can lead to increased times for image capture. This is because invadopodia extending away from the original tumoroid structure now invade in the x-, y-, and z-axes. Therefore, images need to be captured across multiple z-planes to accurately visualize invasion. Increasing the number of images captured, by necessity, also increases the time to capture the image set, and can dramatically increase the hard drive, network, or cloud space required to store the images. To solve this problem, a method to screen wells containing test molecules and the 3D cell model in a rapid way, with decreased storage needs, is desirable. This application note describes a "hit pick" method where the fluorescent signal from test wells was compared to the signal from untreated positive control wells, in order to trigger cellular imaging of "hit" test wells. A FAM-fTHP-9 substrate was developed to serve this purpose. FAM-fTHP-9 is a fluorescently labeled collagen-model synthetic triple-helical peptide substrate designed to be preferentially targeted and degraded by MT1-MMP.[24] MT1-MMP collagenase activity leads to cleavage of the substrate, and an increase in fluorescent signal, detected by the plate reading capabilities of the Agilent BioTek Cytation 5 cell imaging multimode reader.

In the present study, multiple glioma cell lines were formed into tumor spheroids, followed by type I collagen addition. Many known MT1-MMP inhibitors were then added to the wells, to potentially inhibit invasion of the 3D cell models. During the procedure, all control and test wells were read, and the signal from cleaved substrate was quantified. Uninhibited invasion within positive control wells exhibited high fluorescence values. Therefore, a hit pick criterion was established: any wells containing test molecules that were statistically lower than average in fluorescent signal from the corresponding positive control, which should exhibit inhibited invasion, were imaged. Wells that were not significantly lower were not imaged. The result was an easy-to-perform, robust method to reduce image capture time and storage requirements.

Experimental

Materials

Cells

A-172 glioblastoma cells (part number CRL-1620), H4 astrocytoma cells (part number HTB-148), SW 1088 astrocytoma cells (part number HTB-12), and U-87 glioblastoma cells (part number HTB-14) were obtained from ATCC: The Global Bioresource Center (Manassas, VA).

Experimental components

Type I collagen solution from rat tail (part number C3867) and marimastat (part number M2699) were purchased from Sigma-Aldrich (Saint Louis, MO). HyClone fetal bovine serum (part number SH3007103) was sourced from GE Healthcare Life Sciences (Piscataway, NJ). Penicillin-streptomycin (100x) (part number 15140-122) and Hepes, 1 M (part number 15630-080) were purchased from Thermo Fisher Scientific (Waltham, MA). Aprotinin (part number 4139) and recombinant human TIMP-2 protein, CF (part number 971-TM) were purchased from R&D Systems (Minneapolis, MN). The 96-well black/clear round-bottom ultralow attachment spheroid microplates (part number 4515) were purchased from Corning Life Sciences (Corning, NY).

Cytation 5 cell imaging multimode reader

Agilent BioTek Cytation 5 cell imaging multimode reader is a modular, multimode microplate reader, combined with an automated digital microscope. Filter- and monochromator-based microplate reading is available, and the microscopy module provides up to 60x magnification in fluorescence, brightfield, color brightfield, and phase contrast. The instrument can perform fluorescence imaging in up to four channels in a single step. With special emphasis on live-cell assays, Cytation 5 features shaking, temperature control to 65 ºC, CO_2/O_2 gas control, and dual injectors for kinetic assays. It is controlled by integrated Gen5 microplate reader and imager software, which also automates image capture, analysis, and processing. The instrument was used to kinetically monitor the fluorescent signal from the FAM-fTHP-9 substrate, in addition to 3D tumoroid activity, over the incubation period.

Methods

Cell preparation and tumoroid formation

Cells were harvested in a final concentration of 5.0 x 10^4 cells/mL for each cell type in complete medium. After dispensing 200 µL of cell suspension into appropriate microplate wells, the microplates were incubated at 37 ºC/5% CO_2 for 72 to 96 hours, depending on cell type, to allow cells to aggregate into tumoroids.

Invasion matrix preparation

Upon completion of tumoroid formation, 80 to 90% of complete medium was manually removed from each well, and the tumoroid plate was placed on ice in a refrigerator for 5 minutes to cool the cells. The collagen matrix was then thawed on ice. Once thawed, a working solution was then created, such that every 1 mL contained: 750 µL of stock collagen solution, 250 µL of complete cell type appropriate complete media, and 30 µL of 1 M HEPES. With the plate still on ice, 150 µL of collagen working solution was added to each well of the spheroid microplates. Each microplate was centrifuged at 300 ×g for 5 minutes in a swinging bucket centrifuge that was previously set to 4 ºC for tumoroid positioning, then transferred to a 37 ºC/5% CO_2 incubator for 1 hour to initiate gel formation.

Inhibitor and FAM-fTHP-9 substrate addition

Following gel formation, microplates were removed from the incubator and an equal volume of cell-specific complete media was added to the wells, with or without test inhibitors. Final concentrations of inhibitors were: 400 µM marimastat, 4 µM aprotinin, and 30 µM TIMP-2. The plates were once again placed back into the incubator for 1 hour. Finally, FAM-fTHP-9 substrate was added to each well to a final concentration of 5 µM.

Kinetic FAM-fTHP-9 substrate reading and tumor invasion imaging assay performance

Upon addition of the FAM-fTHP-9 substrate, spheroid plates that were used to test the ability of kinetically tracking fluorescent substrate signal and tumoroid invasion were placed into the Cytation 5. A discontinuous kinetic procedure was created to both detect the green fluorescent signal from each well using the Cytation 5 variable bandwidth monochromators, and to capture tumoroid images using the brightfield transmitted light imaging channel. Reading and imaging were carried out every 6 hours over a 48-hour period. Table 1 lists the settings used to perform automated reading and image capture of each sample well.

Table 1. Kinetic FAM-fTHP-9 substrate reading and tumoroid imaging assay parameters.

Temperature	37/2 °C gradient
Monochromator Settings	Ex: 485/20 nm / Em: 528/20 nm
Brightfield Imaging Channel	Complete 3D invading structure
Objective	4x
Z-stack	16 slices
Z-stack Step Size	53.8 µm
Discontinuous Kinetic Total Imaging Time	48 hours
Discontinuous Kinetic Imaging Interval	6 hours

FAM-fTHP-9 substrate reading and tumor invasion imaging hit pick assay performance

Following addition of inhibitor molecules and substrate, as previously described, spheroid plates were placed into a tissue culture incubator for 48 hours. At the end of the incubation period, the plates were transferred into the Cytation 5 to perform the hit pick experiment. The automated procedure consisted of three steps, as shown in Figure 1.

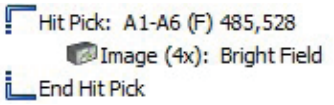

Figure 1. Hit pick multistep process.

In the first step, a fluorescence intensity read was carried out on all appropriate wells of the plate for the cell type being tested with the Cytation 5 monochromators. Settings for the monochromators were the same as those used for the kinetic reading and imaging experiments, shown in Table 1. The top portion of Figure 2 shows the complete set of criteria selected to perform the automated reading step.

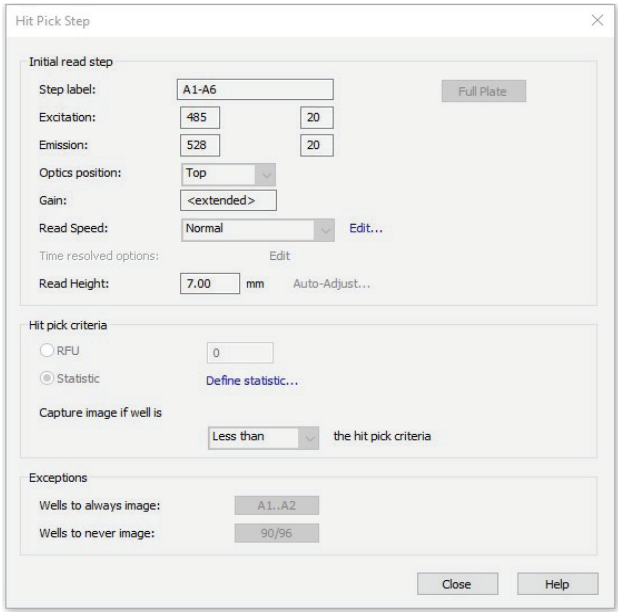

Figure 2. Hit pick read step criteria.

By clicking Define statistic in the Hit Pick Step window, a statistically defined criteria was then determined to trigger test well imaging. The average and standard deviation of the signal from untreated, positive control wells (which should exhibit the highest amount of FAM-fTHP-9 substrate cleavage, and therefore highest signal for each cell type) were automatically calculated by Gen5. The criteria were then set, such that the signal from inhibitor test wells had to be greater than two standard deviations lower than the average signal from the control wells, as seen in Figure 3. If the signal was lower than these cut-off criteria, the test well was imaged. If the signal did not meet the criteria, the well was left unimaged.

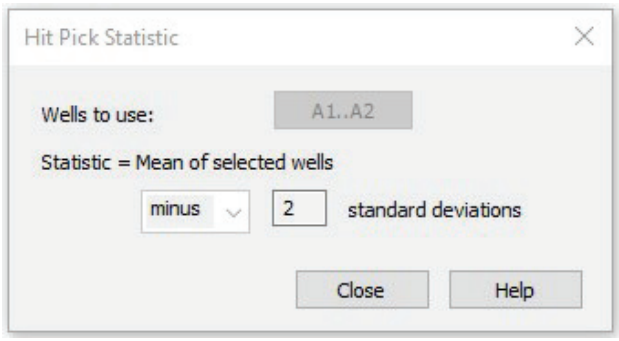

Figure 3. Hit pick statistical criteria.

In the final portion of the “hit pick” procedure, an imaging step was carried out to discern the level of tumoroid invasion following compound incubation, using the brightfield imaging channel. The same imaging settings were again used as those for the kinetic reading and imaging experiments, seen in Table 1. Figure 4 shows the complete set of criteria selected to perform the automated imaging step.

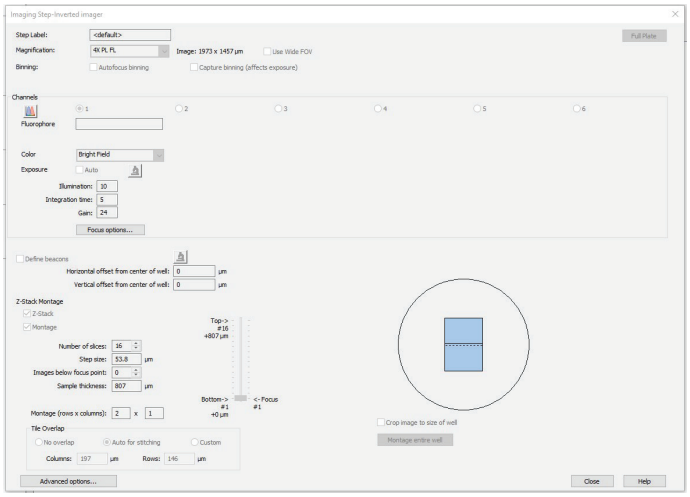

Figure 4. Hit pick imaging step criteria.

Image processing

Individual image tiles from each z-plane captured using the 1 x 2 montage were then stitched together, as shown in Table 2.

Table 2. Image stitching parameters.

Registration Channel	Brightfield
Fusion Method	Linear blend
Crop stitched image to remove black rectangles on the borders	Checked
Downsize Final Image	75%

A single image projection was then created from the 16-slice stitched z-stack, seen in Table 3. The focus-stacking method was chosen, which automatically selects the most in-focus pixel from each image in the stack for inclusion in the final projection. This allows for the most accurate analysis to be carried out on each invading tumoroid at each time point.

Table 3. Image z-projection parameters.

Channel 1	Stitched [Brightfield]
Method	Focus stacking
Size of Maximum Filter	11 px
Z-slice Included	1–16

A signal background removal step was then applied to the stitched, projected images, as shown in Table 4. This served to even out the background brightfield signal and increase the accuracy of cellular analysis mask placement.

Table 4. Image background signal removal parameters.

Background	Light
Rolling Ball Diameter	1200 µm
Image Smoothing Strength	5
Z-slice Included	1–16

Tumoroid invasion analysis

Following image processing, primary cellular analysis criteria (Table 5) were applied using the brightfield channel, to automatically place object masks around the entire invading structure in each final image.

Table 5. Primary mask analysis parameters.

Criteria	A-172	H4	SW 1088	U-87
Channel	Tsf[ZProj[Stitched[Brightfield]]]			
Threshold	7000	6000	4000	7000
Background	Light	Light	Light	Light
Split Touching Objects	Unchecked			
Fill Holes in Masks	Unchecked			
Minimum Object Size	15	300	300	500
Maximum Object Size	2000	5000	5000	2500
Include Primary Edge Objects	Checked			
Analyze Entire Image	Unchecked			
Rolling Ball Diameter	300	1200	750	2000
Image Smoothing Strength	0	5	0	0
Evaluate Background On	5	5	5	20
Metric of Interest	Object sum area			

Results and discussion

Confirmation of FAM-fTHP-9 substrate signal detection

To be able to use the FAM-fTHP-9 substrate in downstream hit pick experiments, it was first necessary to confirm that the signal emanating from the cleaved substrate was strong enough to be detected by the monochromators of the Cytation 5. In addition, it was also imperative that cleaved substrate signal be statistically greater than that detected from wells containing no signal.

An experiment was set up where FAM-fTHP-9 substrate was added to wells, as previously described, containing U-87 tumoroids. No compound was added to these wells. In this manner, the maximum amount of MT1-MMP protease should have been generated in the wells, leading to the largest concentration of cleaved substrate, and highest possible fluorescent signal being emitted. Negative control wells were also set up, where no substrate was added to uninhibited wells containing U-87 tumoroids. The signal from all wells was then quantified every 6 hours over a 36-hour period.

The average signal from positive control wells, containing substrate, was plotted kinetically over time by the Gen5 microplate reader and imager software (Figure 5A, top red line). It is easily seen that the monochromators on the Cytation 5 cell imaging multimode reader could quantify the signal, even when using an embedded 3D tumoroid model. In addition, the quantified signal increased more than 14-fold over time (Figure 5B, top red line), as would be expected when incorporating the highly invasive U-87 glioblastoma cell type. Second, when observing the kinetic curve generated from negative control wells containing no substrate, it can also be seen that little to no fluorescence was detected at any time point during the incubation (Figure 5A, bottom green line). The signal remained stable and did not change in an appreciable manner over time (Figure 5B, bottom green line).

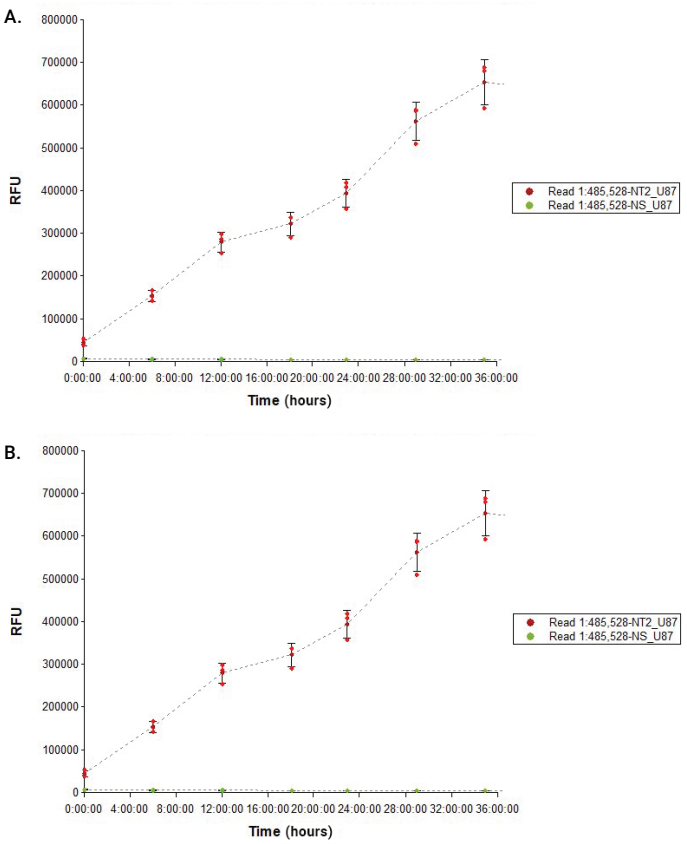

Figure 5. A) Kinetic FAM-fTHP-9 substrate signal from U-87 glioblastoma tumoroids in relative fluorescent units (RFU). B) Normalized substrate signal fold ratio created by dividing signal per time point by signal at time 0.

From the combined results, it is evident that signal from the FAM-fTHP-9 substrate could be accurately detected in a kinetic manner by the Cytation 5 monochromator system, and was statistically greater than background signal.

Increasing FAM-fTHP-9 MT1-MMP substrate signal correlates with increased tumoroid invasion over the same time frame

In the same experiment, where FAM-fTHP-9 substrate signal was kinetically quantified, brightfield images were also captured from wells containing substrate and U-87 tumoroids at the same time points, as shown in Figure 6. When viewing these images, qualitative correlation between increasing substrate signal and tumoroid invasion is apparent.

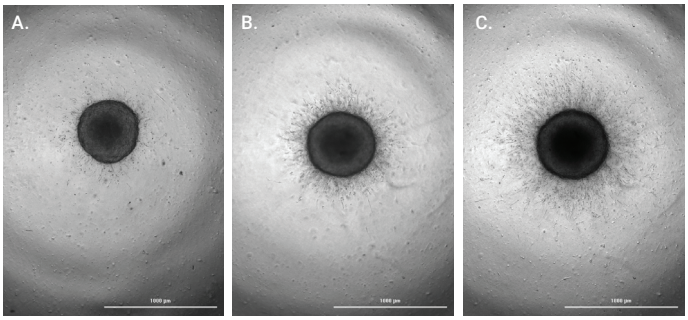

Figure 6. Kinetic 4x brightfield images of U-87 tumoroid invasion after incubation for A) 0 hours, hours; B) 19 hours, hours; and (C) 48 hours.

The correlation between increasing FAM-fTHP-9 substrate signal and increasing tumoroid invasion can also be quantified using the brightfield tumoroid images. Image-processing steps were first applied, including stitching, z-projection, and background removal. Then cellular analysis is applied to the final image using the metrics explained in Table 5. This allows a detailed object mask to be applied to the entire invading structure, as seen in Figure 7.

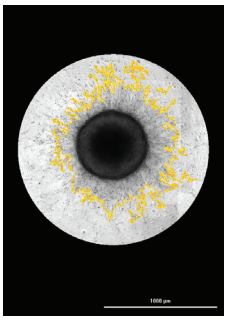

Figure 7. Processed U-87 tumoroid invasion image with cellular analysis object mask applied.

When the curve generated by plotting the kinetic FAM-fTHP-9 substrate fluorescent signal over time (Figure 8A) is compared to the curve created by plotting U-87 tumoroid area coverage over the same time frame, it is apparent that increasing substrate signal was linked to increasing tumoroid invasion into the collagen matrix.

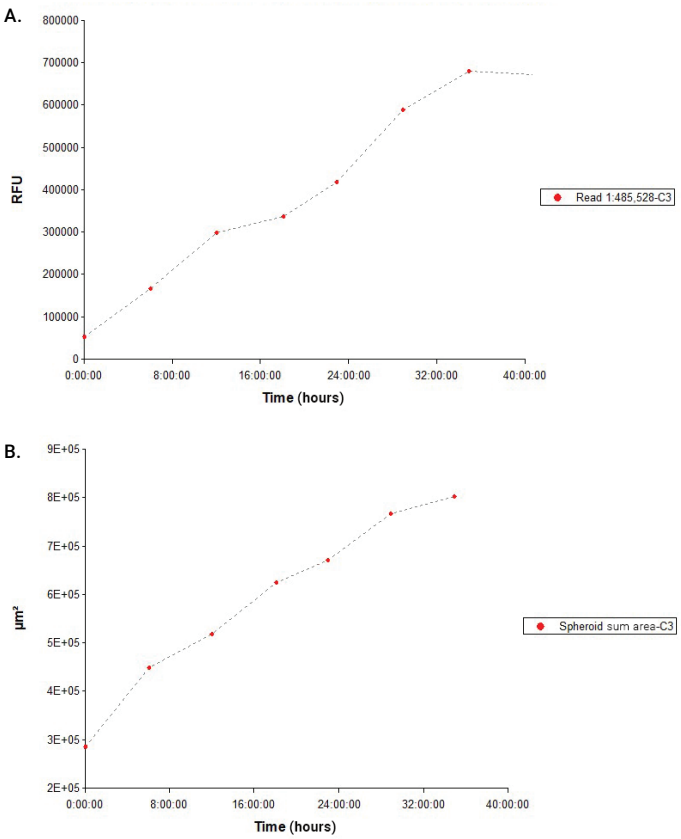

Figure 8. A) Kinetic FAM-fTHP-9 substrate signal from single uninhibited U-87 test well. B) Kinetic tumoroid area coverage from same uninhibited U-87 test well.

Increasing FAM-fTHP-9 MT1-MMP substrate cleavage and resultant signal emanates from MT1-MMP enzyme activity and not from nonspecific cleavage

One of the goals of the project was to create and confidently use a substrate that could assess the activity of MT1-MMP protease in tumoroid invasion. Therefore, in the final confirmatory experiments, it was necessary to ensure that the FAM-fTHP-9 substrate was being cleaved by MT1-MMP, and not from cleavage by other proteases or other means.

To accomplish this task, two experiments were set up. In the first, two known MT1-MMP inhibitors, marimastat and aprotinin, were added to designated test wells containing substrate and U-87 tumoroids. The wells were then read and imaged kinetically in the same manner as previously described, in addition to wells containing uninhibited U-87 tumoroids, and wells containing tumoroids with no substrate.

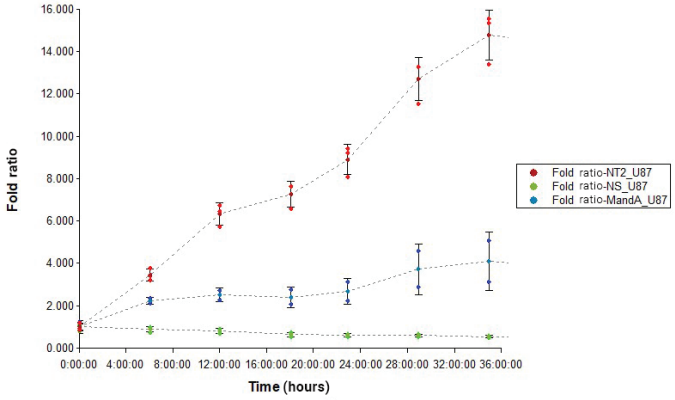

Figure 9. Normalized kinetic substrate signal fold ratio created by dividing signal per time point by signal at time 0. Red curve: uninhibited U-87 tumoroids. Blue curve: 400 µM marimastat and 4 µM aprotinin inhibited U-87 tumoroids. Green curve: U-87 tumoroids with no substrate.

In the second experiment, the substrate was placed in the presence of medium alone, and the signal was read over 48 hours. The average fluorescence detected from these wells, throughout the entire incubation period, was 127 relative fluorescent units (RFU), confirming that the medium contained no inherent ability to cleave the FAM-fTHP-9 substrate.

By observing the results from the experiment in Figure 9, where normalized FAM-fTHP-9 substrate signal is plotted over time, it is evident that wells treated with marimastat and aprotinin together demonstrate a significant decrease in substrate signal over the incubation period. This confirms the specificity of the substrate, as a decrease in signal indicates diminished substrate cleavage from MT1-MMP enzyme activity due to the inhibitory effects of the two MT1-MMP inhibitors. Furthermore, no components in the medium can cause any nonspecific substrate cleavage.

Hit pick assay performance using FAM-fTHP-9 MT1-MMP substrate signal to trigger imaging of test inhibitor wells

A hit pick experiment (Figure 1) was performed to assess the ability of different compounds to inhibit invasion of various 3D glioma cell models through the collagen matrix. As previously described, uninhibited positive control wells were run for each cell type, in addition to the inhibitor containing test wells. A total of 252 wells were included in the experiment across three separate spheroid microplates, including 84 control wells and 168 inhibitor-containing test wells. Following the 48-hour incubation period, where cells were in the presence of substrate and inhibitor or no inhibitor, the fluorescent signal was detected from each well of the spheroid plates (Figure 2). Gen5 software then automatically calculated the average signal from the control wells, in addition to standard deviation. A statistically determined hit pick criteria for each cell type was established to trigger imaging of associated test wells. The criteria stated that if the signal from a test well containing inhibitor exhibited a FAM-fTHP-9 substrate signal lower than the average control well signal, minus two standard deviations (Figure 3), that test well would be imaged using the brightfield imaging step explained in Figure 4. If a test well did not meet these criteria, then the test molecule did not inhibit substrate cleavage to a statistically significant extent, and therefore was not imaged.

Using the criteria established, out of the total 168 inhibitor containing wells tested, 33 wells were unimaged. This is because the substrate signal was not lower than cutoff value, meaning that MT1-MMP activity was not sufficiently inhibited by the test molecule. As a two-image montage and 16-slice z-stack was set to be carried out for each well included, and each brightfield image has a size of 2.1 MB, approximately 17 minutes of imaging time and 2.2 GB of data were saved through incorporation of the hit pick procedure.

The fluorescent substrate signal, and associated images, were then compared between positive control wells per cell type and test inhibitor wells triggered to be imaged, to confirm the validity of the hit pick criteria. This was done for each of the four cell types tested: A-172, H4, SW 1088, and U-87 (Figures 10-13).

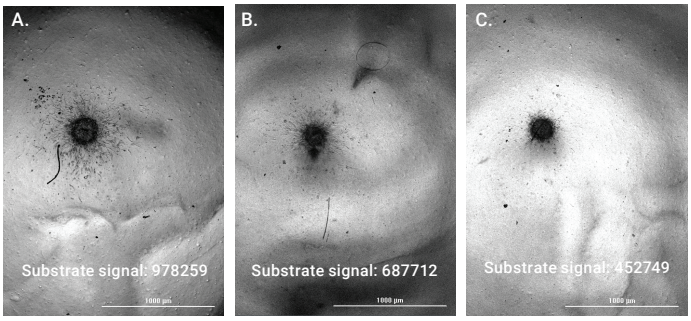

Figure 10. A) A-172 tumoroid; uninhibited. B) A-172 tumoroid; 30 µM TIMP-2 inhibited. C) A-172 tumoroid; 400 µM marimastat, 4 µM aprotinin, 30 µM TIMP-2, 100 µM NSC405020 inhibited.

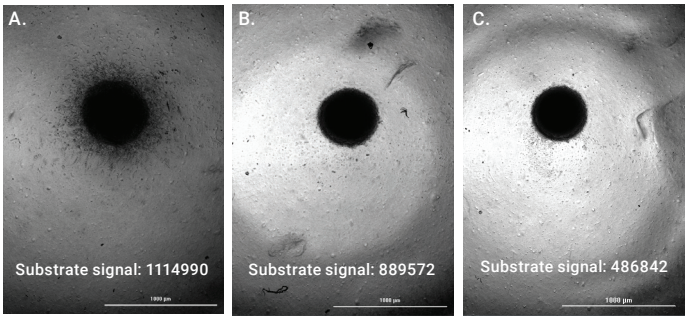

Figure 11. A) H4 tumoroid; uninhibited. B) H4 tumoroid; marimastat, 400 µM inhibited. C) H4 tumoroid; 400 µM marimastat, 4 µM aprotinin, 30 µM TIMP-2, 100 µM NSC405020 inhibited.

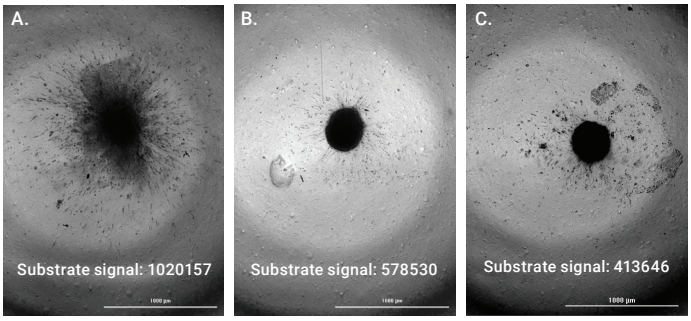

Figure 12. A) SW 1088 tumoroid; uninhibited. B) SW 1088 tumoroid; marimastat, 400 µM inhibited. C) SW 1088 tumoroid; 400 µM marimastat, 4 µM aprotinin, 30 µM TIMP-2, 100 µM NSC405020 inhibited.

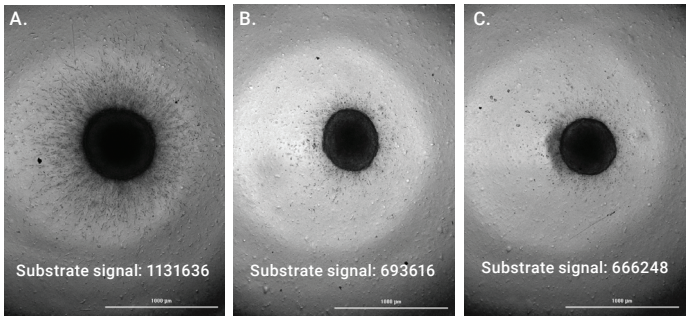

Figure 13. A) U-87 tumoroid; uninhibited; substrate signal. B) U-87 tumoroid; TIMP-2, 30 µM inhibited. C) U-87 tumoroid; 400 µM marimastat, 4 µM aprotinin, 30 µM TIMP-2, 100 µM NSC405020 inhibited.

Upon comparison of the substrate signal with associated images, one can see that inhibitor wells, triggered to be imaged by emitting a lower substrate signal, demonstrated a lower level of tumoroid invasion. The results serve to validate the method as a viable way to quickly screen for inhibitors of glioma tumoroid invasion.

Conclusion

The FAM-fTHP-9 substrate proved to accurately detect MT1-MMP activity of interest. Signal from the cleaved substrate increased over time, proportionately to tumoroid invasion. The substrate itself was also shown to be specific to cleavage from the target MT1-MMP protease, with signal production being reduced accordingly by known MT1-MMP inhibitors. Finally, the combination of the hit picking procedure available in the Agilent BioTek Gen5 microplate reader and imager software, and imaging capabilities of the Agilent BioTek Cytation 5 cell imaging multimode reader, saved significant time and image storage space by only imaging identified inhibitory wells. When combined, the substrate and hit pick process provided an efficient, yet robust method to predict potential inhibitory effects of test molecules on MT1-MMP activity and downstream tumor invasion in 3D glioma cell models.

References

1. *Brain Tumors - Classifications, Symptoms, Diagnosis and Treatments*. https://www.aans.org/. Accessed 24 Oct. **2021**.
2. Ostrom, Quinn T., et al. "CBTRUS Statistical Report: Primary Brain and Central Nervous System Tumors Diagnosed in the United States in 2006-2010." *Neuro-Oncology*, Nov. **2013**, *vol. 15*, no. Suppl 2, pp. ii1–56.
3. Siegel, Rebecca L., et al. "Cancer Statistics, 2021." CA: *A Cancer Journal for Clinicians*, **2021**, *vol. 71*, no. 1, pp. 7–33.
4. Seiki, Motoharu. "Membrane-Type 1 Matrix Metalloproteinase: A Key Enzyme for Tumor Invasion." *Cancer Letters*, May **2003**, *vol. 194*, no. 1, pp. 1–11.
5. Arroyo, A. G., et al. "Matrix Metalloproteinases: New Routes to the Use of MT1-MMP as a Therapeutic Target in Angiogenesis-Related Disease." *Current Pharmaceutical Design*, **2007**, *vol. 13*, no. 17, pp. 1787–802.
6. Itoh, Yoshifumi, et al. "Cell Surface Collagenolysis Requires Homodimerization of the Membrane-Bound Collagenase MT1-MMP." *Molecular Biology of the Cell*, Dec. **2006**, *vol. 17*, no. 12, pp. 5390–99.
7. Itoh, Yoshifumi, and Motoharu Seiki. "MT1-MMP: A Potent Modifier of Pericellular Microenvironment." *Journal of Cellular Physiology*, Jan. **2006**, *vol. 206*, no. 1, pp. 1–8.
8. Xie, Hui, et al. "Expressions of Matrix Metalloproteinase-7 and Matrix Metalloproteinase-14 Associated with the Activation of Extracellular Signal-Regulated Kinase1/2 in Human Brain Gliomas of Different Pathological Grades." *Medical Oncology* (Northwood, London, England), Dec. **2011**, *vol. 28*, Suppl 1, pp. S433-438.
9. Wang, Liang, et al. "Co-Expression of MMP-14 and MMP-19 Predicts Poor Survival in Human Glioma." *Clinical & Translational Oncology: Official Publication of the Federation of Spanish Oncology Societies and of the National Cancer Institute of Mexico*, Feb. **2013**, *vol. 15*, no. 2, pp. 139–45.
10. VanMeter, T. E., et al. "The Role of Matrix Metalloproteinase Genes in Glioma Invasion: Co-Dependent and Interactive Proteolysis." *Journal of Neuro-Oncology*, June **2001**, *vol. 53*, no. 2, pp. 213–35.
11. Sato, Hiroshi, et al. "A Matrix Metalloproteinase Expressed on the Surface of Invasive Tumour Cells." *Nature*, July **1994**, *vol. 370*, no. 6484, pp. 61–65.
12. Hanahan, Douglas, and Robert A. Weinberg. "Hallmarks of Cancer: The next Generation." *Cell*, Mar. **2011**, *vol. 144*, no. 5, pp. 646–74.
13. Hanahan, D., and R. A. Weinberg. "The Hallmarks of Cancer." *Cell*, Jan. **2000**, *vol. 100*, no. 1, pp. 57–70.
14. Yi, Yang, et al. "Glioblastoma Stem-Like Cells: Characteristics, Microenvironment, and Therapy." *Frontiers in Pharmacology*, **2016**, *vol. 7*, p. 477.
15. Tam, Eric M., et al. "Collagen Binding Properties of the Membrane Type-1 Matrix Metalloproteinase (MT1-MMP) Hemopexin C Domain. The Ectodomain of the 44-KDa Autocatalytic Product of MT1-MMP Inhibits Cell Invasion by Disrupting Native Type I Collagen Cleavage." *The Journal of Biological Chemistry*, Oct. **2002**, *vol. 277*, no. 41, pp. 39005–14.
16. Rape, Andrew, et al. "Engineering Strategies to Mimic the Glioblastoma Microenvironment." *Advanced Drug Delivery Reviews*, Dec. **2014**, *vol. 79–80*, pp. 172–83.
17. Bolteus, A. J., et al. "Migration and Invasion in Brain Neoplasms." *Current Neurology and Neuroscience Reports*, May **2001**, *vol. 1*, no. 3, pp. 225–32.
18. Griffith, Linda G., and Melody A. Swartz. "Capturing Complex 3D Tissue Physiology *in Vitro*." *Nature Reviews. Molecular Cell Biology*, Mar. **2006**, *vol. 7*, no. 3, pp. 211–24.
19. Yamada, Kenneth M., and Edna Cukierman. "Modeling Tissue Morphogenesis and Cancer in 3D." *Cell*, Aug. **2007**, *vol. 130*, no. 4, pp. 601–10.
20. Hubert, Christopher G., et al. "A Three-Dimensional Organoid Culture System Derived from Human Glioblastomas Recapitulates the Hypoxic Gradients and Cancer Stem Cell Heterogeneity of Tumors Found *In Vivo*." *Cancer Research*, Apr. **2016**, *vol. 76*, no. 8, pp. 2465–77.
21. Pedron, Sara, et al. "Regulation of Glioma Cell Phenotype in 3D Matrices by Hyaluronic Acid." *Biomaterials*, Oct. **2013**, *vol. 34*, no. 30, pp. 7408–17.
22. Pedron, Sara, et al. "Spatially Gradated Hydrogel Platform as a 3D Engineered Tumor Microenvironment." *Advanced Materials* (Deerfield Beach, Fla.), Mar. **2015**, *vol. 27*, no. 9, pp. 1567–72.
23. Jiguet Jiglaire, Carine, et al. "Ex Vivo Cultures of Glioblastoma in Three-Dimensional Hydrogel Maintain the Original Tumor Growth Behavior and Are Suitable for Preclinical Drug and Radiation Sensitivity Screening." *Experimental Cell Research*, Feb. **2014**, *vol. 321*, no. 2, pp. 99–108.
24. Minond, Dmitriy, et al. "Matrix Metalloproteinase Triple-Helical Peptidase Activities Are Differentially Regulated by Substrate Stability." *Biochemistry*, Sept. **2004**, *vol. 43*, no. 36, pp. 11474–81.

www.agilent.com/lifesciences/biotek

For Research Use Only. Not for use in diagnostic procedures.

RA44622.6331018519

This information is subject to change without notice.

Published in the USA, March 14, 2022
5994-4457EN

Agilent
Trusted Answers